

# New high-spin microsecond isomers in $^{131}\text{Sb}$

 J. Genevey<sup>1,a</sup>, J.A. Pinston<sup>1</sup>, H. Faust<sup>2</sup>, C. Foin<sup>1</sup>, S. Oberstedt<sup>2</sup>, and M. Rejmund<sup>3</sup>
<sup>1</sup> Institut des Sciences Nucléaires, IN2P3-CNRS/Université Joseph Fourier, F-38026, Grenoble Cedex, France

<sup>2</sup> Institut Laue-Langevin, F-38042 Grenoble Cedex, France

<sup>3</sup> DAPNIA/SPhN, CEA Saclay, F-91191 Gif-sur-Yvette Cedex, France

Received: 7 June 2000 / Revised version: 5 September 2000

Communicated by J. Äystö

**Abstract.** In this work we have identified and studied the decay of two new microsecond isomers  $19/2^-$  and  $23/2^+$  in  $^{131}\text{Sb}$ . This neutron-rich nucleus was produced by thermal neutron-induced fission of  $^{241}\text{Pu}$ . The detection is based on time correlation between fission fragments selected by the LOHENGRIN spectrometer at ILL (Grenoble) and the  $\gamma$ -rays or conversion electrons from isomers. These new data on high-spin states complete the level scheme previously obtained from  $\beta$ -decay. A large fraction of the members of the  $\pi g_{7/2}\nu(h_{11/2}^{-1}d_{3/2}^{-1})$  and  $\pi g_{7/2}\nu h_{11/2}^{-2}$  multiplets are now known and were compared with a multi-particle shell model calculation.

**PACS.** 23.20.Lv Gamma transition level energies – 25.85.Ec Neutron-induced fission – 21.60.Cs Shell model – 27.60.+j  $90 \leq A \leq 149$

## 1 Introduction

The nuclide  $^{131}\text{Sb}_{80}$  is of special interest since it has one proton and two neutron holes outside the doubly closed shell nucleus  $^{132}\text{Sn}_{82}$ . Due to its particularly simple structure the results of the particle shell model calculations can be easily compared to the experimental data. However, this neutron-rich nucleus is difficult to produce and the available information concerning its structure comes mostly from  $\beta$ -decay data. In their papers, Stone *et al.* [1, 2] reported an extensive level scheme constructed up to an excitation energy of about 2 MeV. The spins and parities of the levels were firmly established and the members of the  $\pi g_{7/2}\nu(h_{11/2}^{-1}d_{3/2}^{-1})$  and  $\pi g_{7/2}\nu h_{11/2}^{-2}$  multiplets were identified up to the spins  $I^\pi=17/2^-$  and  $I^\pi=11/2^+$ , respectively. The higher-spin members of these two configurations cannot be fed by  $\beta$ -decay and have to be produced via other ways. One possibility is to feed directly by fission the yrast isomers expected to be present among the high-spin levels of the two main configurations. One of these isomers, the  $15/2^-$  state at 1676.7 keV, has been already found [1]. However, the values of the half-lives of this isomer reported in the literature [3–6] scatter between 50 and 95  $\mu\text{s}$ . To remove this ambiguity and to gain more experimental information on the high-spin states of  $^{131}\text{Sb}$ , we have reinvestigated the  $\mu\text{s}$  isomers of this nucleus fed directly by the fission process.

On the theoretical side, the calculations presented in the literature are quite old and incomplete. In the more

recent paper, Heyde *et al.* [7] have performed the one particle-two hole calculations, but the two-body zero-range interaction used for the neutron-proton interaction is too schematic to give sufficiently precise results. Consequently, we have performed a new microscopic shell model calculation up to 2.5 MeV excitation.

## 2 Experimental procedure

The details concerning the experimental set-up are given in [8,9]. The fission fragments of the  $A = 131$  mass chain were produced by thermal neutron induced fission of  $^{241}\text{Pu}$ . The spectrometer LOHENGRIN at ILL has been used to separate the fission fragments of ionic charge  $q = 23$  or 24 recoiling from a thin target of about  $400 \mu\text{g cm}^{-2}$ . The fission fragments were detected by a  $\Delta E$  gas-detector of 13 cm length, and subsequently stopped in a mylar window of 12  $\mu\text{m}$  thickness. The  $\gamma$ -rays decaying the isomeric states were detected by two large volume Ge detectors and the conversion electrons were detected by two cooled Si(Li) detectors covering a total area of  $2 \times 6 \text{ cm}^2$  and located 7 mm behind the mylar window. The gas pressure of the ionization chamber was tuned to stop the fission fragments at about 2  $\mu\text{m}$  from the outer surface of the mylar window to minimize electron absorption and to have a good energy resolution. Events were stored on a disk each time a Si(Li) or a Ge detector was fired within a time window of 40  $\mu\text{s}$  after the implantation of a fission fragment. In this case, the possible  $\gamma$ - $\gamma$ ,

<sup>a</sup> e-mail: genevey@isn.in2p3.fr

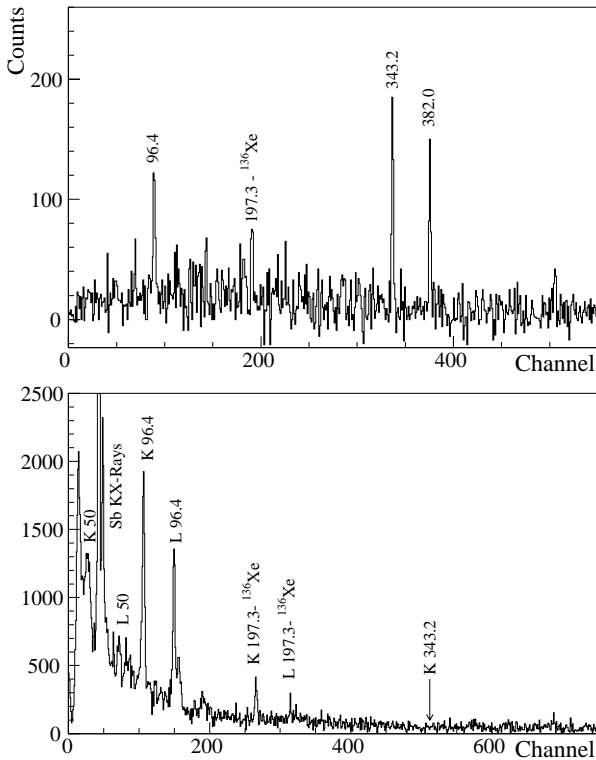


**Fig. 1.**  $\gamma$  and electron spectra of the  $A = 131$  mass chain in delayed coincidence with the fission fragments. The time window  $\Delta T$ :  $0.3\text{--}2.5\ \mu\text{s}$  is too short to observe the 450.3 and 1226.4 keV lines de-exciting the 1676.7 keV isomer. A weak contamination of  $^{136}\text{Xe}$  is due to their close  $A/q$  values. The arrow shows the expected position of the  $K$  343.2 keV line.

$\gamma$ -electron, and electron-electron coincidences detected in a time window of  $4\ \mu\text{s}$  were registered.

### 3 Experimental results

The  $\gamma$  and electron spectra measured in delayed coincidences with the fission fragments of the  $A = 131$  mass chain are shown in fig. 1. Three new  $\gamma$ -rays of 96.4, 343.2 and 382.0 keV have been observed. The Si(Li) spectrum in coincidence with the 343.2 and 382.0 keV  $\gamma$ -rays is shown in fig. 2. Both of these transitions are coincident with lines interpreted as the Sb K X-rays and the  $K$  and  $L$  conversion lines of the 96.4 keV transition observed in the  $\gamma$  spectrum. Moreover, an electron line is also observed below the X-rays in coincidence only with the 343.2 keV transition and is interpreted as the  $K$  conversion line of a 50.0(5) keV transition. The  $L$  line is also seen, but with a much smaller intensity. All these lines have a half-life of  $1.1(2)\ \mu\text{s}$  as seen in fig. 3, where the time decay of the  $K$ -96.4 keV line is reported.

The experimental conversion coefficient  $\alpha_K=1.2(2)$  measured for the 96.4 keV line is compatible only with an  $E2$  assignment. As the  $\gamma$ -ray of the 50 keV transition was not observed, one cannot deduce an  $\alpha_K$  value in this case, but the value  $K/L \sim 6$  measured makes only  $E1$

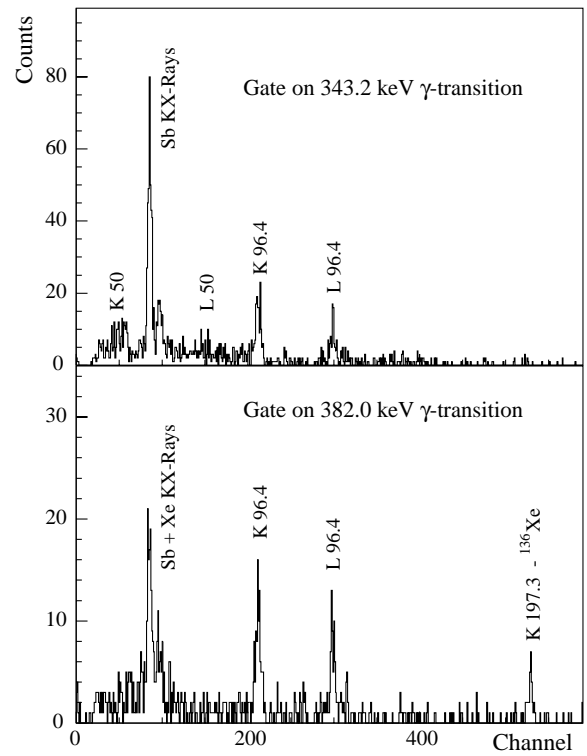


**Fig. 2.** Si(Li) spectrum gated by the 343.2 and the 382.0 keV  $\gamma$ -transitions.

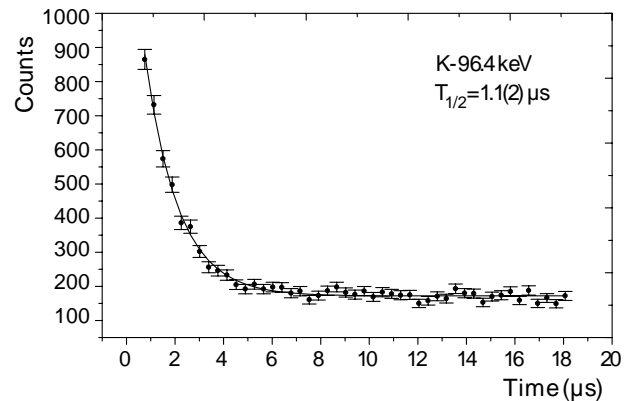


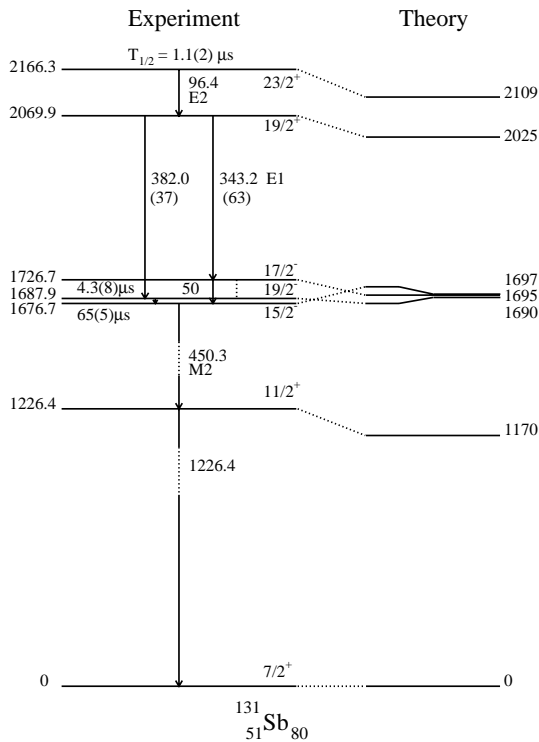
**Fig. 3.** Half-life spectra of the  $K$ -96.4 keV electron-ray.

or  $M1$  assignment possible. Since the  $K$ -line of the 343.2 keV transition was not observed in the delayed spectrum of fig. 1, this suggests an  $E1$  multipolarity for this transition.

At this point of the discussion, one may conclude that a new  $1.1\ \mu\text{s}$  isomer has been observed in the  $^{131}\text{Sb}$  nucleus. As from theoretical considerations (see discussion below and table 1) no levels are expected below the  $\pi d_{5/2}$  state at 798.5 keV, the  $1.1\ \mu\text{s}$  isomer cannot feed directly the ground state, otherwise one would have several states too close to the ground state. In contrast, it can decay on the previously known  $15/2^-$  isomeric state at 1676.7 keV. However, in this case, the half-life of more than  $50\ \mu\text{s}$  previously measured [3–6], prevents the observation of

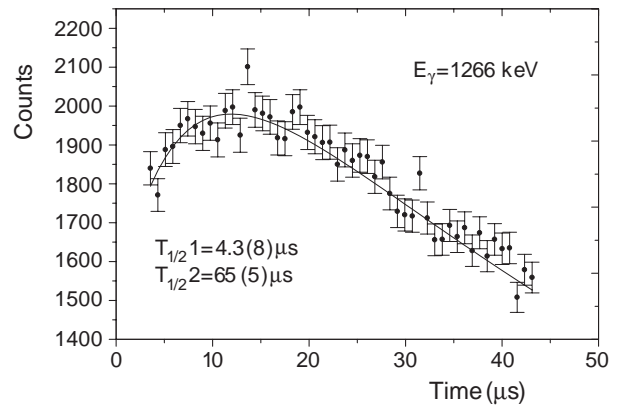
**Table 1.** Experimental and calculated positive- and negative-parity levels in  $^{131}\text{Sb}$ .

$E$ (keV) Expt.	$J^\pi$	$E$ (keV) Calc.	$E$ (keV) Expt.	$J^\pi$	$E$ (keV) Calc.
0	$7/2^+$	0	1872.8	$1/2^+$	1853
798.6	$5/2^+$	$d_{5/2}$	1889.8	$11/2^-$	1986
1141.9	$3/2^+$	1117	1917.4	$15/2^-$	1855
1203.0	$5/2^+$	1089	1931.3	$9/2^+$	
1226.4	$11/2^+$	1170		$13/2^+$	1963
1229.6	$9/2^+$	1394	1981.2	$13/2^-$	1939
1481.2	$7/2^+$	1631	1998.0	$9/2^-$	1916
1676.7	$15/2^-$	1697	2069.9	$19/2^+$	2025
1687.9	$19/2^-$	1690	2166.3	$23/2^+$	2109
1726.6	$17/2^-$	1695		$17/2^+$	2171
1731.0	$13/2^-$	1737		$21/2^+$	2328
1786.9	$3/2^+$			$21/2^-$	2602
1813.4	$11/2^-$	1857		$25/2^+$	2734
	$15/2^+$	1871		$27/2^+$	3485
1871.9	$7/2^-$	1913			

**Fig. 4.** Proposed level scheme of  $^{131m}\text{Sb}$ .

coincidences between the 1.1  $\mu\text{s}$   $\gamma$ -rays and the 450.3 and 1226.4 keV lines de-exciting the  $15/2^-$  isomer. These considerations allow us to construct the level scheme shown in fig. 4. Moreover, the 50.0 keV transition de-exciting the 1726.7 keV level is very likely the same as the one previously measured by Stone *et al.* [1], from the  $\beta$ -decay of the  $11/2^-$  isomer of 58.4 s half-life in  $^{131}\text{Sn}$ . A spin and parity  $I^\pi=17/2^-$  was already assigned to this state.

The time spectrum measured for the 1226.4 keV and 450.3 keV transitions is characteristic of the subsequent

**Fig. 5.** Half-life spectra of the 1226.4 keV  $\gamma$ -ray.

decay of two isomeric states. The case of the 1226.4 keV transition is shown in fig. 5. The unfolding of the decay curve allows to extract the values  $T_{1/2}(1) = 4.3(8) \mu\text{s}$  and  $T_{1/2}(2) = 65(5) \mu\text{s}$  for the half-lives and the relative fission yields of 35% and 65% for the short and long components, respectively. This new result shows for the first time the existence of two half-lives, and this explains the large spread of the values of the previously measured half-lives [3–6]. One should note that this half-life has never been measured in  $\beta$ -decay experiments but only in delayed coincidence work with fission products.

This new half-life of 4.3  $\mu\text{s}$  is very likely associated with the 1687.9 keV state, expected to decay by a non-observed, very low-energy isomeric transition of 11.2 keV. Its reduced transition probability, assuming an  $E2$  multipolarity, is  $B(E2)=0.99(18)$  W.u. This suggests that the isomeric transition takes place between two levels having a large  $E2$  overlap of their wave functions and that the new isomer at 1687.9 keV should have a spin and parity  $I^\pi=19/2^-$ . To confirm this hypothesis, we have compared the transition probability measured in  $^{131}\text{Sb}$  with the the  $15/2^- \rightarrow 19/2^-$  transition in  $^{129}\text{Sb}$ . One should note that the initial and final spins are inverted in  $^{129}\text{Sb}$  and  $^{131}\text{Sb}$ . For this purpose, we have measured the half-life of the  $15/2^-$  state in  $^{129}\text{Sb}$ , already observed at 1851.3 keV [1]. From the measured value  $T_{1/2} = 2.2(2) \mu\text{s}$ , the value  $B(E2)=1.90(17)$  W.u. was deduced for the direct  $15/2^- \rightarrow 19/2^-$  transition and  $B(E2)=1.52(14)$  W.u. for the reversed transition  $19/2^- \rightarrow 15/2^-$ . The last value is rather close to the analogous one for  $^{131}\text{Sb}$ .

The 2069.9 keV state decaying by an  $E1$  transition to the  $19/2^-$  and to the  $17/2^-$  state but not to the  $15/2^-$  has a spin and parity  $I^\pi=19/2^+$ , while the 2166.3 keV one decaying by an  $E2$  transition has a spin and parity  $I^\pi=23/2^+$ . The isomeric transition rate,  $B(E2)=0.53(10)$  W.u., suggests that here also the transition takes place between levels having a large  $E2$  overlap.

The  $17/2^-$  state at 1726.7 keV could also decay to the new  $19/2^-$  state at 1687.9 keV by a low energy  $M1$  transition of 38.8 keV. However, it is difficult to observe experimentally its conversion electrons, because the  $K$ -line of 8.3 keV is below the detection limit of the Si(Li) detector and the  $L$ -line of 34 keV is expected to be too weak

**Table 2.** Experimental and calculated  $B(E2)$  transition probabilities in  $^{131}\text{Sb}$ .

Transition	$T_{1/2}$ $\mu\text{s}$	$B(E2)$ ( $e^2\text{fm}^4$ )	
		Expt.	Calc.
$23/2^+ \rightarrow 19/2^+$	1.1(2)	21(4)	24.1
$19/2^+ \rightarrow 15/2^+$			42.5
$19/2^- \rightarrow 15/2^-$	4.3(8)	40(7)	38.6

and too close to the  $K_\beta$  X-rays to be observed without ambiguity. One should note that this transition was not reported in the paper of Stone *et al.* [1].

## 4 Comparison with theory

### 4.1 Energy levels

A semi-empirical shell model calculation was performed using the code OXBASH [10]. A truncated configuration space was used including only the valence orbitals  $g_{7/2}$  for the protons and  $d_{3/2}$  and  $h_{11/2}$  for the neutrons. The numerical calculations have been performed using the particle-particle formalism. The single-particle energies relative to  $^{132}\text{Sn}$   $E(\pi g_{7/2}) = -9633$  keV and  $E(\nu d_{3/2}) = +7325$  keV, were deduced from the measured masses of  $^{133}\text{Sb}$  and  $^{131}\text{Sn}$  [11]. The  $\nu h_{11/2}$  single particle level is suggested to be placed 110 keV above the  $\nu d_{3/2}$  level, as discussed in ref. [9]. The two body matrix elements of the residual interaction were extracted, wherever possible, from experimental data. However, complete experimental data are not available on the  $\pi g_{7/2}\nu h_{11/2}$  multiplet, and therefore we have used the calculated values of Andreozzi *et al.* [12].

In this calculation the  $s_{1/2}$  neutron orbital measured at 332 keV above the  $d_{3/2}$  ground state level in  $^{131}\text{Sn}$  [13] is not explicitly introduced because its interactions with the  $h_{11/2}$ ,  $d_{3/2}$  neutrons and  $g_{7/2}$  proton are not known experimentally. However, the experimental matrix elements which are employed include implicitly effects of the possible configuration mixing with the  $s_{1/2}$ . Thus, it is expected that the shortcomings of the shell model without configuration mixing, are compensated by using experimental effective interactions that already contain high-order corrections.

The comparison between the known experimental levels of  $^{131}\text{Sb}$  and the calculation is shown in table 1 and in the level scheme of fig. 4. In our calculation  $^{131}\text{Sb}$  is overbound by 114 keV. Consequently, the calculated energies of the levels displayed in table 1 and fig. 4 are given relative to the calculated ground state. The first  $5/2^+$  state measured experimentally at 798.5 keV as well as the second  $3/2^+$  at 1786.9 keV and  $9/2^+$  at 1931.3 keV cannot be computed with this simple model because in these states the proton occupies mainly the  $d_{5/2}$  orbital, not used in the calculation. A reasonable agreement between the calculated and the experimental energies is evident in fig. 4 and table 1. The calculated  $23/2^+$  state is well below the

$21/2^+$  state and becomes yrast. It can only decay by a low energy  $E2$  transition to the  $19/2^+$  and this explains its experimentally measured long half-life.

The  $15/2^-$ ,  $17/2^-$  and  $19/2^-$  states of the  $\pi g_{7/2}\nu(h_{11/2}^{-1}d_{3/2}^{-1})$  multiplet are reproduced with a precision of the order of 30 keV (2 %). This figure, rather good for a shell model calculation, is, however, not sufficient to reproduce the order of these levels: the  $15/2^-$  state is the lowest observed state of the configuration while theory predicts it to be the  $19/2^-$  state. The consequences of this feature are dramatic: instead of one long-lived predicted isomer decaying by  $\beta$  emission as in  $^{129}\text{Sb}$ , two  $\mu\text{s}$  isomers of 65 and 4.3  $\mu\text{s}$  were observed experimentally. This striking result shows the necessity of new and more precise model calculations in this mass region. It is then a challenge for theoreticians to perform sophisticated calculations in the future, including all necessary orbitals, and using various theoretical interactions.

### 4.2 Transition rates

The  $B(E2)$  reduced transition probabilities obtained from the present experiment are compared with our theoretical predictions in table 2. The effective polarization charges  $e_{\text{pol}}^\pi = 0.9 \cdot e$  and  $e_{\text{pol}}^\nu = 0.9 \cdot e$  were extracted from the experimentally known  $B(E2, \pi g_{7/2}^2, 6^+ \rightarrow \pi g_{7/2}^2, 4^+)$  in  $^{134}\text{Te}$  and  $B(E2, \nu h_{11/2}^{-2}, 10^+ \rightarrow \nu h_{11/2}^{-2}, 8^+)$  in  $^{130}\text{Sn}$  [14,15], respectively. It is clear from table 2, that the reduced transition probabilities calculated with the present approach reproduce very well the experimental data.

The  $19/2^+$  state of  $\pi g_{7/2}\nu h_{11/2}^{-2}$  configuration decays by two competing  $E1$  transitions to the  $19/2^-$  and  $17/2^-$  members of the  $\pi g_{7/2}\nu(h_{11/2}^{-1}d_{3/2}^{-1})$  multiplet. In fact, the  $E1$  transitions are strongly forbidden between the main configuration of the corresponding states and therefore they proceed via small admixtures of other configurations. The other possibility to depopulate the  $19/2^+$  state would be by the stretched  $E2$  transition to the  $15/2^+$  state of the same configuration. This state is predicted by the model to be 154 keV lower in excitation energy than the  $19/2^+$  state. However, this transition was not observed in the present experiment implying that its relative intensity is lower than 5% and a large  $H_W \leq 2 \cdot 10^6$  W.u. hindrance factor was deduced for the two  $E1$  transitions. For a similar  $E1$  decay, *i.e.*  $\nu(h_{11/2}^{-1}d_{3/2}^{-1})(5^-) \rightarrow \nu h_{11/2}^{-2}(4^+)$  in  $^{130}\text{Sn}$ , a hindrance of  $2.3(2) \cdot 10^5$  W.u. was measured [14].

## 5 Conclusions

In this paper we have identified and studied the decay of the two new  $19/2^-$  and  $23/2^+$  isomers. These new data substantially extend our knowledge of this neutron-rich nucleus to higher-spin states and a large fraction of the states of the two  $\pi g_{7/2}\nu(h_{11/2}^{-1}d_{3/2}^{-1})$  and  $\pi g_{7/2}\nu h_{11/2}^{-2}$  configurations are now identified. This allows a detailed comparison with theory. For this purpose a microscopic shell

model calculation was performed assuming a truncated configuration space. The main features of the level scheme are well reproduced by the model and the  $23/2^+$  isomer is well predicted. The excited energy of the new  $19/2^-$  isomer is also well predicted.

We thank M. Asghar for comments and a careful reading of the manuscript.

## References

1. C.A. Stone, S.H. Faller, J.D. Robertson and W.B. Walters, *Proceedings of the 5<sup>th</sup> International Conference on Nuclei far from Stability, Rosseau Lake, Canada, 1987*, edited by I.S. Towner (AIP, New York, 1988) p. 429.
2. C.A. Stone, D. Robertson, S.H. Faller, P.F. Mantica, B.E. Zimmerman, C. Chung and W.B. Walters, *Phys. Scr. T* **56**, 316 (1995).
3. R.B. Walton and R.E. Sund, *Phys. Rev.* **178**, 1894 (1969).
4. R. Sellam, thesis, University of Grenoble, 1976; F. Schussler, J. Blachot, J.P. Bocquet and E. Monnard, *Z. Phys. A* **281**, 229 (1977).
5. B. Proot and J. Uyttenhove, *Nucl. Instrum. Meth.* **192**, 447 (1982).
6. J.W. Borgs, H.P. Kohl, G. Lhersonneau, H. Ohm, U. Paf-frath, K. Sistemich, D. Weiler and R.A. Meyer, *Nucl. Instrum. Meth. B* **26**, 304 (1987).
7. K. Heyde, J. Sau, R. Chery, F. Schussler, J. Blachot, J.P. Bocquet, E. Monnard and K. Sistemich, *Phys. Rev. C* **16**, 2437 (1977).
8. J.A. Pinston, C. Foin, J. Genevey, R. Béraud, E. Chabanat, H. Faust, S. Oberstedt and B. Weiss, *Phys. Rev. C* **61**, 024312 (2000).
9. J. Genevey, J.A. Pinston, C. Foin, H. Faust, S. Oberstedt and B. Weiss, *Eur. Phys. J. A* **7**, 463 (2000).
10. B.A. Brown, A. Etchegoyen, W.D.H. Rae, OXBASH (1984) unpublished.
11. B. Fogelberg, K.A. Mezilev, H. Mach, V.I. Isakov and J. Slivova, *Phys. Rev. Lett.* **82**, 1823 (1999).
12. F. Andreozzi, L. Coraggio, A. Covello, A. Gargano, T.T. S. Kuo and A. Porino, *Phys. Rev. C* **59**, 272 (1995).
13. B. Fogelberg and J. Blomqvist, *Phys. Lett. B* **137**, 20 (1984).
14. B. Fogelberg, K. Heyde and J. Sau, *Nucl. Phys. A* **352**, 157 (1981).
15. A. Kerek, G.B. Holm, S. Borg and L.-E de Geer, *Nucl. Phys. A* **195**, 177 (1972).